VERSITA

Arch. Min. Sci., Vol. 58 (2013), No 2, p. 521–540

Electronic version (in color) of this paper is available: http://mining.archives.pl

DOI 10.2478/amsc-2013-0035

TIAN-RANG JIA*,**, ZI-MIN ZHANG**, CHUN-AN TANG*[1], YONG-JUN ZHANG***

NUMERICAL SIMULATION OF STRESS-RELIEF EFFECTS OF PROTECTIVE LAYER EXTRACTION

SYMULACJA NUMERYCZNA SKUTKÓW ODPRĘŻENIA WARSTWY ZABEZPIECZAJĄCEJ W TRAKCIE JEJ WYBIERANIA

Field test and laboratory analog model test on the stress-relief effects of protective layer extraction are time-consuming and laborious. In this paper, on the basis of full consideration of rock heterogeinity and in combination with gas geology at Pingdingshan Mine 5, a numerical model was estalished with the gas-solid coupling rock failure process analysis system RFPA-Gas to simulate the stress variation law, roof and floor deformation, fracture evolution law, displacement in the protected seam, change in gas permeability and gas migration law during protective layer extraction. The simulation results repoduced stress variations in coal and rock strata, roof and floor deformation and fracture evolution process during protective layer extraction. The movement of rock strata were characterized by upper three zones and lower two zones: caving zone, fracture zone and bending subsidence zone in the vertical direction in the overlying strata; floor deformation and failure zone and elasto-plastic deformation zone in the vertical direction in the underlying strata. It showed that stress relief occurred in the protected seam, which led to vertical and horizontal displacements, significant increase in gas permeability, gas desorption and migration. Hence, the outburst threat in the protected seam was eliminated. Meanwhile, with comprehensive analysis of variaition of stress state, deformation characteristics and fracture distribution in coal seam and with consideration of changes in gas leakage rate, gas pressure and permeability, according to gas leakage rate, the floor strata of the protecive layer were divided into four leakage zones. They corresponded to four zones with different stress states and fracture development: original leakage zone - slow reducing leakage zone – dramatic increasing leakage zone– steady increasing leakage zone. This classification provides a clear direction for gas control in the protective layer. The simulation results are in good agreement with the stress-relief effects in field.

Keywords: protective layer, stress relief, numerical simulation, leakage zones

* INSTITUTE OF ROCK INSTABILITY AND SEISMICITY RESEARCH, DALIAN UNIVERSITY OF TECHNOLOGY, DALIAN 116024, LIAONING, PR CHINA

** INSTITUTE OF GAS GEOLOGY, HENAN POLYTECHNIC UNIVERSITY, JIAOZUO 454003, HENAN, PR CHINA

*** SCHOOL OF CIVIL ENGINEERING, QINGDAO TECHNOLOGICAL UNIVERSITY, QINGDAO 266033, SHANDONG, PR CHINA

[1] CORRESPONDING AUTHOR. E-mail: tca@mail.neu.edu.cn

Badania terenowe oraz modelowanie w warunkach laboratoryjnych skutków odprężenia warstwy zabezpieczającej w trakcie wydobycia są niezwykle czasochłonne i skomplikowane. Uwzględniając niejednorodność skał i wykorzystując dane geologiczne i o obecności gazów w kopalni Pindingshan 5, opracowano model numeryczny pękania skał w układzie gaz-ciało stałe w oparciu o analizę układu RFPA-Gaz. Model wykorzystano do symulacji zmian naprężeń, odkształceń stropu i spągu, propagacji pęknięć, przemieszczeń w pokładach zabezpieczonych, zmian w przepuszczalności gazów oraz migracji gazów w trakcie wybierania warstwy zabezpieczającej. Wyniki symulacji odwzorowują zmiany naprężeń, odkształceń stropu i spągu, propagacji pęknięć w trakcie wybierania warstwy ochronnej. Ruchy warstw górotworu scharakteryzowano poprzez analizę trzech stref nadkładu i dwóch stref lezących poniżej: w warstwach nadkładu: strefy zawału, strefy spękań oraz strefy osiadania (przemieszczenia w kierunku pionowym), w warstwach leżących poniżej: strefy odkształcenia i pękania spągu, oraz strefy odkształceń elastyczno- plastycznych w kierunku pionowym. Wykazano, że odprężanie miało miejsce w pokładzie zabezpieczającym, co prowadziło do powstania przemieszczeń pionowych oraz poziomych, zanotowano także znaczny wzrost przepuszczalności gazów, desorpcji gazów oraz ich transportu. Z tych względów zagrożenie wybuchem w pokładzie ochronnym zostało wyeliminowane. Całościowa analiza zmian stanu naprężenia, charakterystyki odkształceń i rozkładu pęknięć w pokładzie węgla przeprowadzona została dla czterech stref przecieku gazów, wydzielonych w oparciu zmiany natężenia wypływu gazów, ciśnienia gazów oraz przepuszczalności w odniesieniu do natężenia przepływu gazu w spągu w warstwie ochronnej. Te cztery strefy odpowiadały czterem strefom w których zanotowano odmienne stany naprężeń i rozkładu spękań: pierwotna strefa wycieku, powoli zmniejszająca się strefa wycieku, gramatycznie powiększająca się strefa wycieku i stopniowo powiększająca się strefa wycieku. Powyższa klasyfikacja dostarcza wyraźnych wytycznych dla prowadzenia kontroli wycieku gazu w warstwach ochronnych. Wyniki symulacji skutków odprężania wykazują dużą zgodność z wynikami badań terenowych.

Słowa kluczowe: warstwa ochronna, odprężanie, symulacje numeryczne, strefa wycieku

1. Introduction

For coal mines prone to gas outburst, extraction of a protective layer is one of the most economic and effective ways to prevent coal and gas outburst in adjacent coal seams (Yu, 2004). The protective layer is a pre-excavated coal or rock seam in order to eliminate the outburst threat in adjacent coal seams. Extraction of the protective layer results in intensive tensile failure in the overlying and underlying strata. The overlying coal strata may be caved, fractured, subsided or bent; the underlying stratum may be cracked or heaved. A large amount of fractures in coal strata open up, and at the same time, numerous new fractures are formed. Geo-stresses are released effectively in a large extent and the gas permeability increases by hundred or even thousand times. Gas pressure deceases dramatically and hence a great deal of desorbed gas leaks into the working face of the protective layer. In this way, the gas outburst threat in the protected seam is eliminated (Jia, 2006). However, it is extremely difficult to evaluate the protection effect in terms of field monitoring of the roof and floor stress and displacement of the protective layer, the gas permeability of the protected seam, gas pressure, and the dynamic evolution of gas leakage volume with mining of the protective layer. Analog model tests in laboratory can be very time-consuming and laborious as well. Numerical simulation can overcome the deficiency of field tests and model tests.

According to fracture development and permeability, Gaiduk divided the surrounding rock masses within the naturally-balanced arch into irregularly-displaced zone, caving zone, fractured-displaced zone and unfractured-displaced zone (Elune, 1992). Coalescent permeable fractures formed an integrated permeable system in the irregularly-displaced zone and the caving zone. The desorbed gas in the fractured-displaced zone can run through the coalescent fractures, however,

no integrated permeable system was formed. The residual gas pressure was small and depended on the original pressure. The permeability in the unfractured-displaced zone was not improved evidently. Gas can not flow from the protective layer to the protected seam along the fractures. The gas emission and outburst threat in the protected seam were slightly changed locally. The residual gas pressure was determined by the original pressure. Literature investigated the effects of the protective layer in gently inclined coal seams by finite element method (Yang et al., 1988). It was found that after extraction of the protective layer, stress concentration zone, stress relief zone and intact stress zone were formed in the overlying rock strata. By field inspection and statistical analysis, Kuznetsov pointed out the effective role of the protective layer, proposed a zoning method of the protected range according to the stress in the rock pillar above the first outburst depth and obtained the variation law of stress relief effect with stratum spacing (Yang, 1992). Cheng Y.P. et al. (2003) proposed a long-distance gas extraction method which conformed to gas flow characteristics in remote strata under stress relief. Shi B.M. et al. (2004), Liu Z.G. and Yuan L. (2006), and Yang T.H. et al. (2004) conducted numerical simulations on fracture evolution and change in gas permeability during protective layer extraction. The previous researches have been primarily focused on fracture evolution and changes in gas permeability induced by protective layer extraction. So far, no study, which evaluates the protection effect of the protective layer by considering gas-solid coupling and based on comprehensive analysis of stress variation in the protected strata, displacement in rock strata, changes in gas permeability, flow volume and gas pressure, has been reported. In this paper, taking gas geology at Pingdingshan Mine 5 as background, RFPA-Gas program is adopted to evaluate the protection effect. The simulation results are compared with the stress-relief effects in the field, and the good agreement are verified between simulation and measured results.

2. Model establishment

The gas-solid coupling model mainly includes three types of equation respectively for gas leakage filed, coal deformation and permeability-damage evolution.

2.1. Equation for gas leakage field

Gas movement in coal follows the linear leakage law. If taking coal gas as ideal gas and leakage as an isotherm process, according to gas state equation and mass conservation law, the leakage field equation for gas movement in coal can be obtained (Yang et al., 2004):

$$\alpha_p(\lambda_i \nabla^2 P) = \frac{\partial P}{\partial t} \tag{1}$$

where $\alpha_p = 4A^{-1}P^{\frac{3}{4}}$; λ_i is permeability coefficient ($m^2/(MPa^2 d)$); P is the square of gas pressure (MPa^2), $P = p^2$, p is gas pressure in coal seam (MPa). A is the gas content in coal seam ($m^3/(m^3 \cdot MPa^{1/2})$).

2.2. Equation for coal deformation

Taking gas pressure into account, the equation for coal deformation can be expressed in term of displacement (Liu & Yuan, 2006):

$$(\kappa + G)\, u_{j,ji} + G u_{i,jj} + f_i + (\alpha p)\, i = 0 \tag{2}$$

where G and κ are, shear modulus and *Lamé* constant, respectively; u is displacement; $i, j = 1, 2, 3$; f_i is physical strength per unit volume (MPa); α is coefficient for gas pressure and $0 < \alpha < 1$.

2.3. Equation for permeability-damage evolution

Under mining disturbance, coal undergoes deformation and damage. When the stress or strain state in a micro-element reaches a certain threshold value, damage occurs. Correspondingly, the element permeability also changes. Based on this idea, the evolution relationship between permeability coefficient and damage can be established (Valliappan & Zhang, 1996).

The Mohr-Coulomb criterion is adopted to be the failure criterion for elements. When the shear stress reaches the damage threshold, the damage variable D can be expressed as

$$D = \begin{cases} 0 & (\varepsilon < \varepsilon_{c0}) \\ 1 - \dfrac{\sigma_{cr}}{E_0 \varepsilon} & \varepsilon_{c0} \le \varepsilon_r \end{cases} \tag{3}$$

where σ_{cr} is the compressive residual strength and the subscript r denotes residual; ε_{c0} is the maximum compressive strain; ε_r is the residual strain.

The corresponding element permeability can be expressed in the following form:

$$\lambda = \begin{cases} \lambda_0 e^{-\beta(\sigma 1 - \alpha p)} & (D = 0) \\ \xi \lambda_0 e^{-\beta(\sigma 1 - \alpha p)} & (D > 0) \end{cases} \tag{4}$$

where λ_0 is the original permeability coefficient; p is gas pressure ξ, α, β are magnification factor for permeability coefficient, gas pressure coefficient and stress influencing (coupling) coefficient, respectively.

Similar law can be applied to the permeability-damage coupling equation for coal micro-elements under uniaxial tension. When the tensile stress in an element reaches the damage threshold value for tensile strength, the damage variable D is in the form of

$$D = \begin{cases} 0 & (\varepsilon \le \varepsilon_{t0}) \\ 1 - \dfrac{f_{tr}}{E_0 \varepsilon} & (\varepsilon_{t0} \le \varepsilon < \varepsilon_{tu}) \\ 1 & (\varepsilon_{tu} \le \varepsilon) \end{cases} \tag{5}$$

The corresponding element permeability can be expressed as:

$$\lambda = \begin{cases} \lambda_0 e^{-\beta(\sigma_3 - \alpha p)} & (D = 0) \\ \xi\lambda_0 e^{-\beta(\sigma_3 - \alpha p)} & (0 < D < 1) \\ \xi'\lambda_0 e^{-\beta(\sigma_3 - \alpha p)} & (D = 1) \end{cases} \tag{6}$$

where f_{tr} is the tensile residual strength and the subscript t denotes tension; ξ' is magnification factor for permeability coefficient when damage occurs in the element.

Equations (1), (2), (4) and (6) constitute the solid-gas coupling mathematical model for gas flow in coal.

2.4. Model establishment

2.4.1. Physical model

Coal seam group mining is adopted in Pingdingshan mining area. The coal seams are divided into four major groups from bottom up, namely, Taiyuan Group G, Shanxi Group F, Xiashihezi Group E and Shangshihezi Group D. For Mines 3, 4, 5, 6, 7, 11 and 13 in the west of the mining area under Group F, the thickness of coal seam F_{15} is about 1.5 m and not exposed to gas outburst threat. Coal seam F_{15} is about 1.0-20 m away from seam $F_{16,17}$, which is generally 3.5 m or above in thickness and prone to serious gas outburst. If Seam F_{15} is taken as the upper protective layer, gas in seam $F_{16,17}$ can be effectively released and gas outburst threat can be eliminated. The pilot area was chosen at F_{15} - 23220 working face in Section 3 of Mine 5. This layer was excavated as the protective layer to protect the underlying $F_{16,17}$ - 23220 working face. The F_{15} - 23220 working face was 1100 m in strike length, and 190 m in dip length. The ventilation lane was 810-890 m below ground surface and the cover depth for the roadway was 845-941 m. The coal seam F_{15} is 1.5 m thick in average and its gas content was 7.0 m^3/t. The underlying protected $F_{16,17}$ - 23220 working face has a seam thickness of 3.5 m, gas content of 18 m^3/t, gas pressure of 2.1 MPa and original permeability coefficient of 0.002 m^2/MPa^2d. The mechanical properties for rock strata are listed in Table 1.

TABLE 1

Mechanical parameters for rock strata at Pingdingshan Mine 5

Lithology	Density (kg/m^3)	Thickness (m)	Elastic modulus E (GPa)	Poisson's ratio ν	Compressive strength (MPa)	Friction angle (°)	Ratio of compressive and tensile strength
1	2	3	4	5	6	7	8
Equivalent block 1	60000	15	15000	0.4	120	37.5	8
Equivalent block 2	40000	15	18000	0.32	150	36	8
Sandstone 1	2300	20	10000	0.25	100	32	9
Sandstone 2	2350	20	12000	0.28	110	35	9
Sandstone 3	2450	20	9000	0.26	95.6	36.2	9
Fine sandstone	2750	10	8500	0.32	90	34	9

1	2	3	4	5	6	7	8
Siltstone	2510	20	7000	0.35	75	34.7	10
Fine-grain sandstone	2630	15	10000	0.27	110	38	11
Sandy mudstone	2250	15	6500	0.32	70	36.5	11
Medium-grain sandstone	2470	15	8000	0.29	85	32	12
Sandy mudstone	2350	6	5600	0.31	50	36.1	10
Coal seam F_{15}	1550	1.5	1800	0.39	20	31	10
Sandy mudstone	2650	5	5800	0.28	40	28.5	10
Fine-grain sandstone	2500	2	8000	0.3	50	30	10
Sandy mudstone	2900	2	6000	0.35	50	35	10
Coal seam $F_{16,17}$	1800	4	2200	0.38	25	32	9
Mudstone	2600	2	2620	0.31	35	29.5	10
Sandy mudstone	3100	7	5150	0.36	68	37.1	10
Marlite	2610	2	3200	0.34	55	36	10
Sandy mudstone	2900	5	6000	0.31	78	35	10
Sandstone	3100	20	7500	0.35	85	35	10
Sandstone floor	3200	35	12000	0.28	128	31	10

2.4.2. Numerical model

On the basis of full consideration of rock heterogeneity and the constitutive relation at microscopic scale, and with the gas geology at Pingdingshan Mine 5 as background, a two-dimensional plane strain model was established for numerical simulation, as shown in Fig. 1. The numerical model was 400 m in the horizontal direction and 280 m in the vertical direction. The 22 rock strata were divided into 112000 (400 × 280) elements. In view of the weak planes in real rock strata, some bedding planes were set in the model.

Longwall top caving method was adopted for coal mining and no support was installed. The model boundary conditions were set as follows: self-weight along the vertical direction, fixed end constraint in the horizontal direction and fixed at the bottom. The grey scale in the figure denoted different elastic moduli of rock strata. The lighter the grey color, the greater the elastic modulus. The open-off cut was at 150 m to the right boundary and 10 m coal was mined for each step. Due to the limited capacity of the model, for the overlying rock strata with thickness more than 750 m, material with equivalent bulk density was used for the top two layers. Each layer was 15 m in thickness and the total thickness was then 30 m. In order to avoid influence of damage of heavy blocks on rock stratum movement, the material strength was increased.

The mechanical properties of each rock stratum (elastic modulus, strength of element and etc.) conform to Weibull distribution, where m is the shape parameter reflecting the degree of homogeneity of mechanical properties of rock material. The larger the m value is, the more homogeneous the rock is.

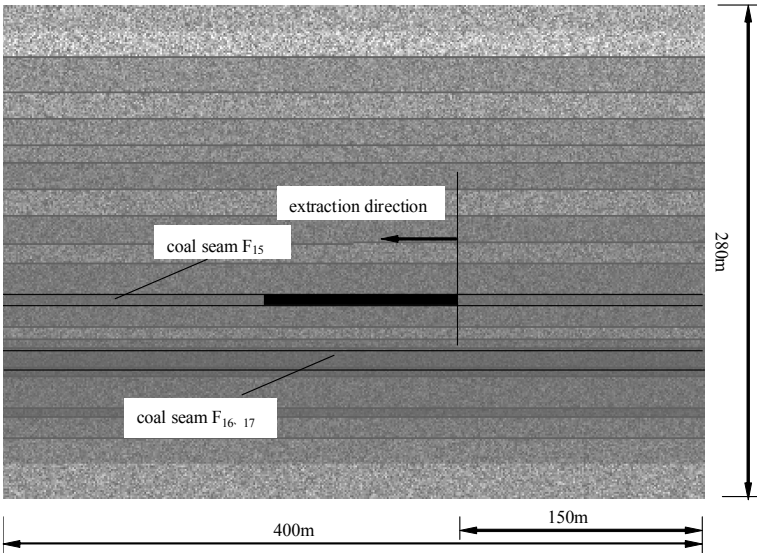

Fig. 1. Sketch of RFPA model

3. Evaluation of stress-relief effects

3.1. Deformation, damage and fracture evolution laws in the protective layer

The deformation process in the roof and floor strata, the top caving process and the corresponding distribution of elastic moduli during extraction of the protective layer are shown in Fig. 2. The dynamic development of damage zone is illustrated in Fig. 3. It can be seen from Fig. 2, with advance of the working face, the roof stratum deformed first, and bed-separation fractures were observed in the top and middle parts of the roof stratum immediately above the excavated area. Bending and subsidence occurred due to gravity (The color for acoustic emission is mainly red). The ends of rock beam cracked. When the working face was advanced by 25-30 m, a "pseudo-plastic rock beam" was formed as the rock beam cracked in the center. As the immediate roof for coal seam F_{15} mainly consisted of sandy mudstone, which was very stable, top caving was not likely to occur. At the same time, tensile and shear damage was observed in the floor stratum near the open-off cut (The color for acoustic emission was white and red). Cracks extended from the bottom of coal wall to the deep floor below goaf area in a step-wise manner, accompanied by bed separation. When the working face was advanced by 30 m, the corresponding distribution of elastic moduli is shown in Fig. 2 and damage zones in Fig. 3.

It shows "upper three zones" in the overlying strata and "lower two zones" during extraction of the protective layer, namely, caving zone, fractured zone, and sagging zone in the overlying strata; deformation and failure zone and elastic-plastic deformation zone in the floor strata. Their locations can be seen from Fig. 4.

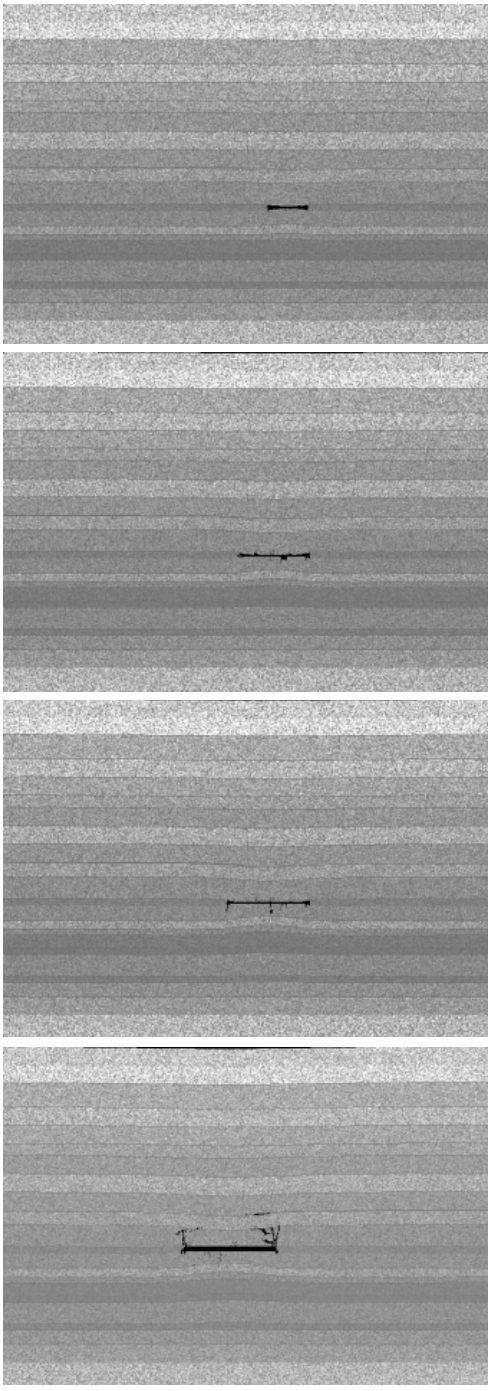

Fig. 2. Distribution of elastic moduli during extraction of protective layer

Fig. 3. Distribution of damage zone during extraction of protective layer

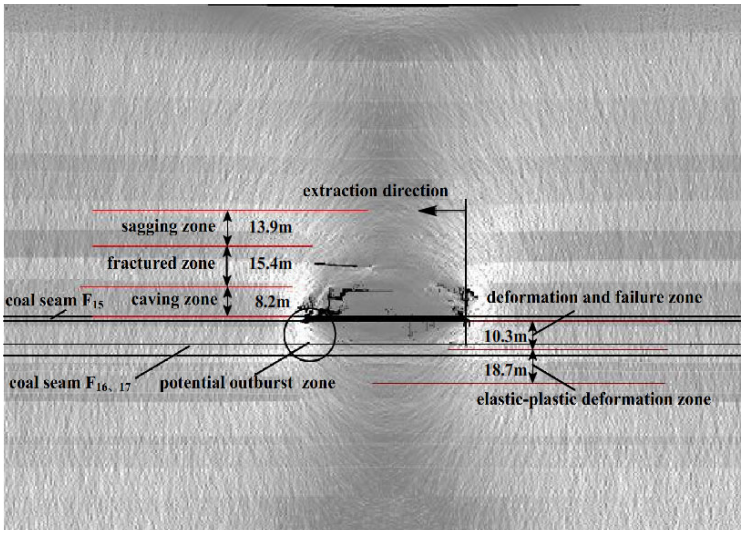

Fig. 4. Sketch of "upper three zones" in the overlying stratum and "lower two zones" in the floor stratum

Floor heave occurred as well as large vertical cracks. In fact, it was a complex fracture network. The local amplified view shown in Fig. 5 can help to visually determine the magnitude and nature of fracture-inducing stresses. From the distribution of stresses and fractures during recovery of the protective layer, we can see that at the junction of the compression and expansion zones, the floor was prone to tensile-shear failure. A large amount of tensile-shear fractures initiated and coalesced to connect the protective layer and the protected seam. Channels were then created for gas flow. The gas leakage rate and volume increased. When the thickness of the underlying rock strata is less than 2m or faults exist, coal and gas outburst are likely to take place.

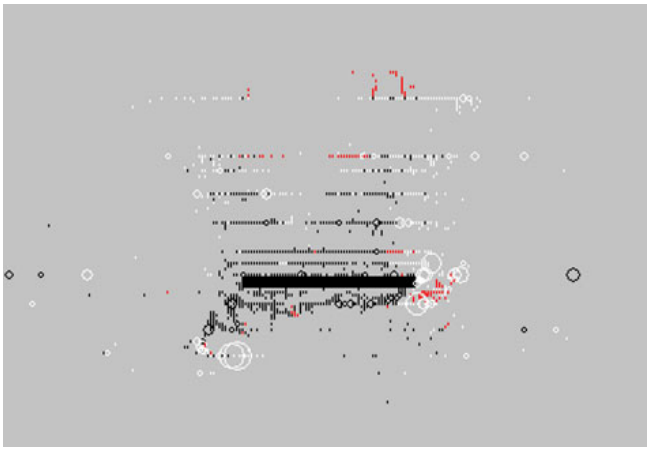

Fig. 5. Local amplified view of fracture network

3.2. Stress variation in the protective layer and the protected seam

The deformation process in the roof and floor strata, the top caving process and the corresponding dynamic evolution of principal stress and shear stress during extraction of the protective layer are shown in Figs. 6 and 7, respectively. The numerical modeling results show that:

(1) The bearing pressure was small in the coal wall near the working face due to mining-induced stress relief. The overall trend of the bearing pressure along the direction away from the mining area was that it rose to the peak value first, and then decreased until it reached in-situ stress. Meanwhile, the variation trend of the principal stress in the protected seam $F_{16,17}$ was consistent, reflecting the scope and extent of stress relief in the protected seam, as illustrated in Fig. 6.

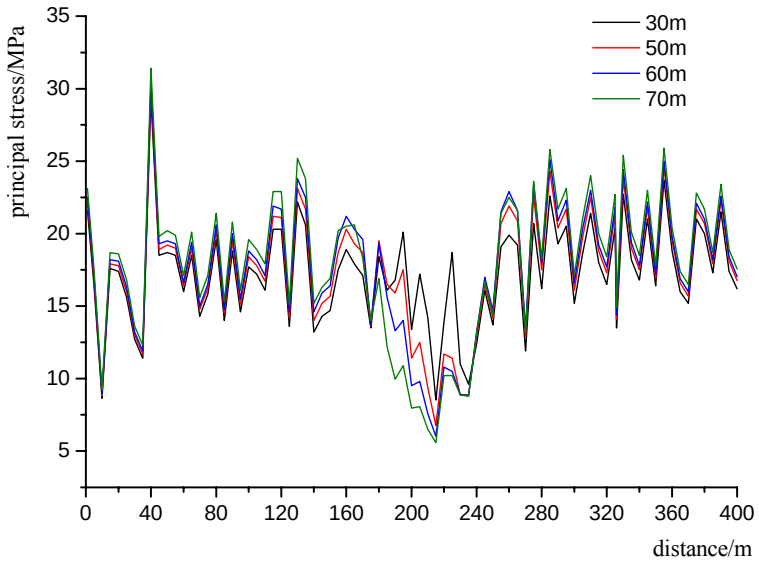

Fig. 6. Distribution of principal stress in seam $F_{16,17}$ during extraction of protective layer

(2) When the working face was further advanced, the goaf area gradually increased. The overlying rock strata originally carried by the coal in goaf area was then supported by the coal wall. More fractures appeared in rock beam above the goaf. Damage occurred in the coal seam behind coal wall.

(3) The floor strata deformed under ground pressure. The deformation in the vertical direction can be divided into two portions from bottom up: the upper deformation and failure zone and the lower elasto-plastic deformation zone. The rock structure in the deformation and failure zone was damaged under ground pressure and its continuity was greatly reduced. Strata-parallel and vertical fractures occurred and the permeability increased remarkably. The influencing area was about 8-12 m below coal seam F_{15}. The majority of the

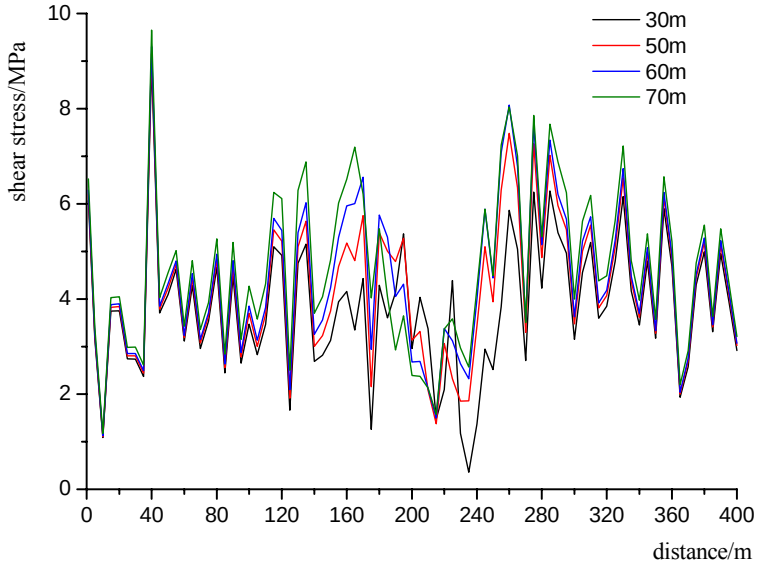

Fig. 7. Distribution of shear stress in seam $F_{16,17}$ during extraction of protective layer

protected coal seam $F_{16,17}$ was within this area. Therefore, the permeability coefficient increased significantly, even by more than 2000 times. The lower elasto-plastic deformation zone was loaded by ground pressure. Elastic or plastic deformation and fractures may occur. However, its continuity was basically maintained as the same before mining and fractures were not coalescent. The permeability coefficient underwent relatively small change. It can be divided into two sub-zones, dominated by plastic deformation and elastic deformation, respectively. Under the impact of mining-induced stresses, the elasto-plastic deformation zone was within the range of 15-20 m below the deformation and failure zone in the floor stratum.

(4) With advance of the working face, the weight of overlying strata supported by coal pillar gradually increased. The concentrated bearing pressure in the coal pillar kept rising. The concentration coefficient of bearing pressure increased gradually. As a result, coal and rock strata in the vicinity of the stress concentration point became plastic and the bearing capacity was reduced. Hence, the stress concentration point moved backwards, in another word, the distance between the stress concentration point and the working face gradually increased. Meanwhile, tensile stresses in the floor stratum led to floor heave, which resulted in stress relief, fracture growth and higher permeability in the protected seam $F_{16,17}$.

From Figs. 6 and 8, it can be seen that stress concentrated in a certain range in coal seams $F_{16,17}$ near the open-off cut. With continuous advance of the working face, the concentrated stress increased gradually. The location for stress concentration below the open-off cut in the protected seam extended further toward the corresponding location above goaf in the protective layer. An elasto-plastic high stress zone was formed within 12 m coal between the open-off cut and the coal pillar. The bearing pressure and shear

stress were the highest in this region, which reached 30 MPa and 9.8 MPa, respectively. Compressive-shear failure occurred in coal stratum and fracture channels were formed. Compared to other regions, the difference in gas pressure between coal seam and goaf was the largest in this region. Hence, gas outburst was likely to occur and this region was the potential outburst area in coal seam $F_{16,17}$, corresponding to the locations indicated in Figs. 2(d) and 3(d).

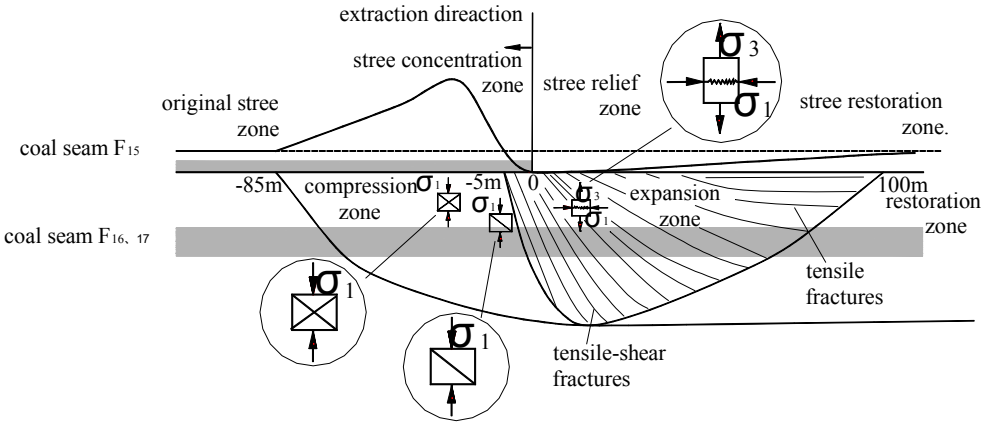

Fig. 8. Sketch of stress zones in the protective layer and fracture distribution in the floor stratum

(5) Normally, during extraction of the protective layer, the floor strata underwent the repeated process of stress increase (compression) – stress relief (expansion) – stress restoration with advance of the working face. When the working face passes, the stress reached the peak value and the minimum stress was 14-50 m behind the working face. At this moment, fractures were most developed in the floor strata and gas in the protected seam flowed into goaf areas in the protective layer.

(6) According to the theory of ground pressure and simulation results, the stress distribution in the roof can be divided into four zones: original stress zone, stress concentration zone, stress releif zone and stress restoration zone. The stress in the floor is redistributed due to mining disturbance and can be divided into normal stress concentration zone, stress relief zone and stress restoration zone in plane. Correspondingly, the deformation in the floor can be divided into compression zone, expansion zone and restoration zone, as illustrated in Fig. 8. At the junction of the compression and expansion zones, tensile-shear failure occurred and a large amount of tensile-shear fractures formed in the floor stratum. Bed-separation and vertical fractures were likely to form in the expanded floor stratum. These fractures provided comminucation channels between the protective layer and the protected seam. A large quantity of desorbed gas flowed from the protected seams into the protetive layer. Therefore, this region is very important for gas control in the protective layer.

3.3. Deformation and displacement in the protected seam

The dynamic evolution of vertical and horizontal displacements in the protected seam $F_{16,17}$ during extraction of the protective layer are shown in Fig. 9 and 10, respectively. In the figures, the horizontal axis stands for the horizontal position in the model and the vertical axis for the displacement in the protected seam $F_{16,17}$. The sign convention in Fig. 9 is that vertically downward displacement is positive, and in Fig. 10 is that horizontal displacement toward the advancing direction is positive. When excavated to 30 m, the deformation in the protected seam was small. The maximum vertical displacement was 51.2 mm and the maximum horizontal displacement

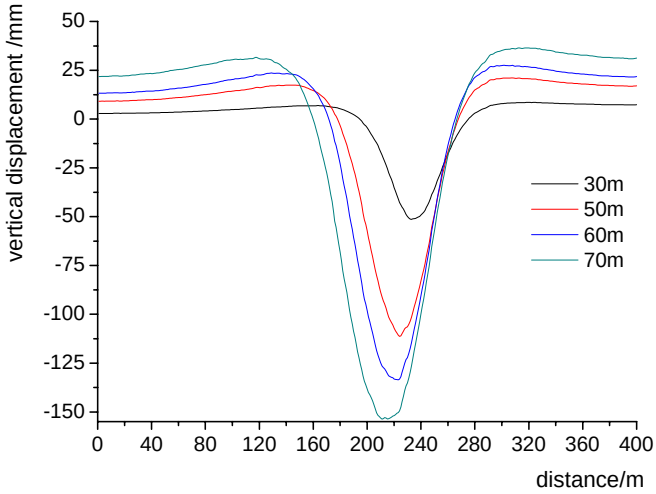

Fig. 9. Distribution of vertical displacement in seam $F_{16,17}$ during extraction of the protective layer

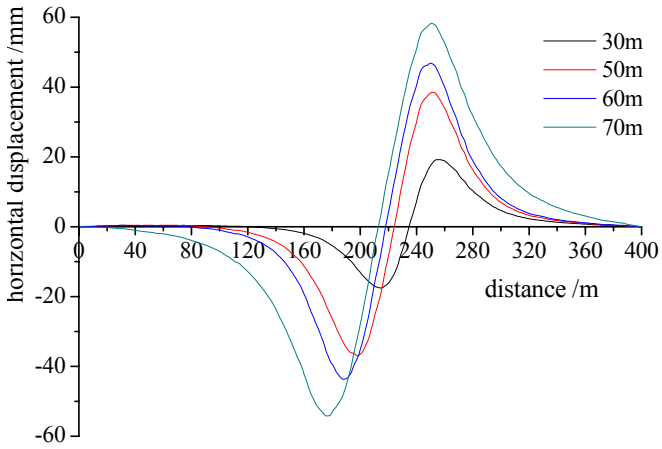

Fig. 10. Distribution of horizontal displacement in seam $F_{16,17}$ during extraction of the protective layer

toward the goaf area was 19.2 mm. When the working face advanced by 50 m, 60 m and 70 m, the corresponding maximum vertical displacements in the protected seam were 111 mm, 133 mm and 154 mm, respectively; the maximum horizontal displacements were 38 mm, 46.3 mm and 58.2 mm, respectively. With advance of the working face, the deformation in the protected seam underwent the process of compression – expansion – reduced expansion until steady state.

3.3. Permeability and gas migration in the protected seam

During extraction of the protective layer, the protected seam expanded due to stress relief. A large amount of bed-separation fractures and inter-seam fractures were formed. Gas in the protected seam desorbed due to stress relief and flowed into the protective layer through fracture channels driven by gas pressure gradient. By this way, the outburst threat in the protected seam was eliminated. Figs. 11 to 13 plot the distribution of gas permeability coefficient, gas flow in the vertical directions and gas pressure in the protected seam $F_{16,17}$. By comparison between Figs 11 to 13, the gas pressure gradient was relatively large near the open-off cut and the working face from the initial mining stage to advance by 50-60 m. The stress in the coal wall was not released. The permeability was reduced by some amount. The corresponding gas flow amount was small. However, the stress in the floor stratum below the goaf area was released. The elastic energy was released and floor heave and tensile fractures occurred. Gas permeability was increased and gas pressure decreased rapidly. Correspondingly, gas volume was relatively large. This is called "stress relief and gas flow increase effect". When the working face was advanced by 60-70 m, gas permeability increased significantly in the deformation and failure zone in the floor stratum. Gas pressure gradient became large and the shear fracture channel below the coal wall was formed. The gas pressure decreased rapidly in this zone. At the same time, the leakage rate and gas volume also rose rapidly. Gas outburst was likely to occur, as illustrated in Figs. 12 and 13. After the working face was advanced by 70 m, the gas pressure in the protected seam

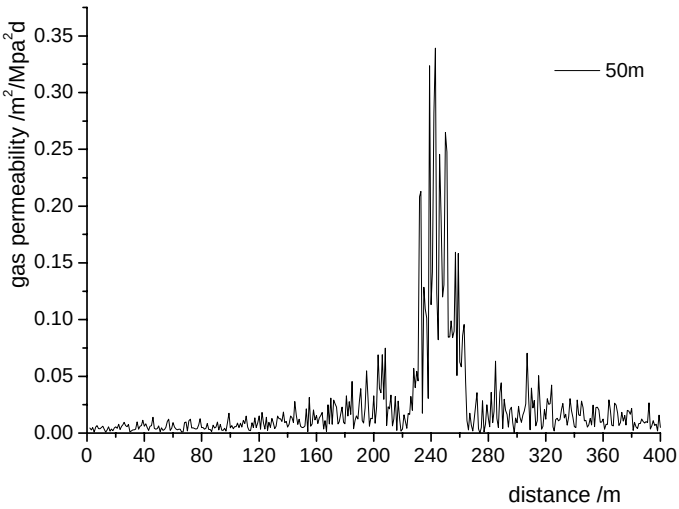

(a) Distribution of gas permeability in seam $F_{16,17}$ when advance by 50 m

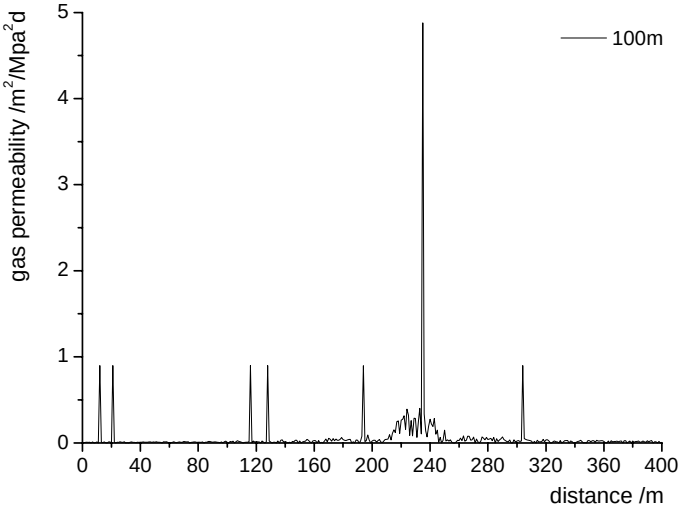

(b) Distribution of gas permeability in seam $F_{16,17}$ when advance by 100 m

Fig. 11. Distribution of gas permeability in seam $F_{16,17}$ during extraction of the protective layer

$F_{16,17}$ was reduced to less than 0.6 MPa, which was 28.6% of the original gas pressure (2.1 MPa). When advanced by 100 m, the gas permeability coefficient rose to 5m^2/MPa^{2}d in the protected seam, which was 2500 times of the original permeability coefficient (0.002 m^2/MPa^{2}d). If gas was extracted when the protective layer was mined, the gas content would be even lower in the protected seam and the potential gas outburst can be completely eliminated.

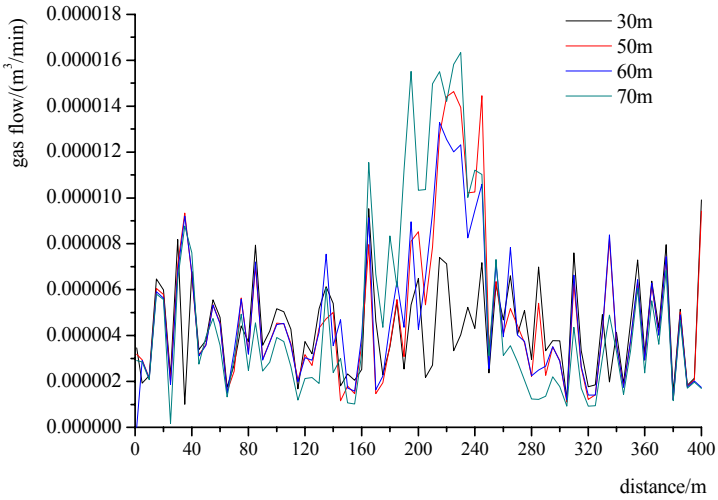

Fig. 12. Distribution of gas flow in vertical direction in seam $F_{16,17}$ during extraction of the protective layer

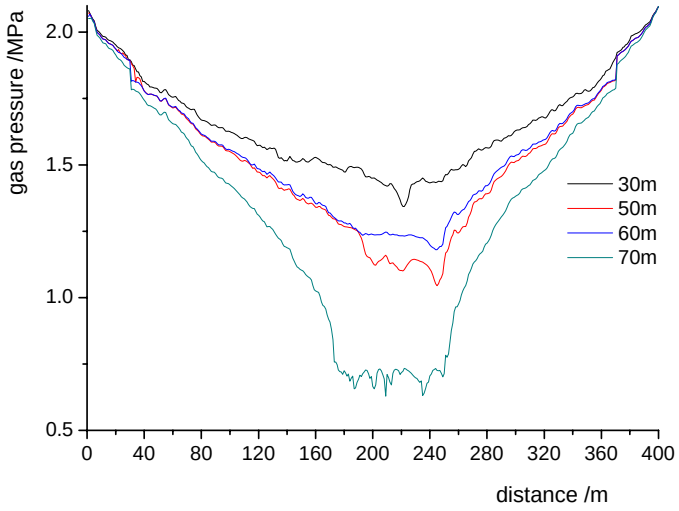

Fig. 13. Distribution of gas pressure in seam $F_{16,17}$ during extraction of the protective layer

3.4. Zoning of gas seepage in the floor strata under the protective layer

By comprehensive analysis of stress variation (Figs. 6-8), deformation characteristics (Figs. 9 and 10) and fracture distribution (Figs. 3-5), and with consideration of gas seepage rate, gas pressure (Figs. 12 and 13) and variation of gas permeability (Figs. 11 and 14), according to gas

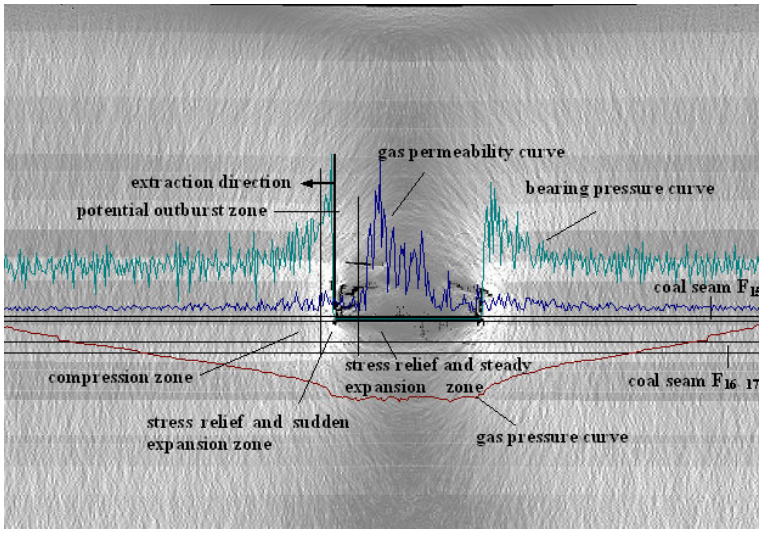

Fig. 14. Stress distribution zones and permeability coefficient in the protected layer

leakage rate, the floor stratum under the protecive layer can be divided into four leakage zones (Fig. 15). They corresponded to four zones with different stress states and fracture development: original leakage zone (original stress zone) – slow reducing leakage zone (stress concentration zone) – dramatic increasing leakage zone (stres relief and sudden expansion zone) – steady increasing leakage zone (stress relief and steady expansion zone). Among them, the stress relief and sudden expansion zone referred to the region between the vertical fracture and horizontal bed separation fracture in the floor, i.e., the region between the compressive-shear fracture below coal wall and micro-fracture in the goaf area. Under large gas pressure gradient, this region is highly prone to gas outburst. The stress relief and steady expansion zone was located in the horizontal fracure zone due to floor heave, correspoding to tensile failure zone in the floor.

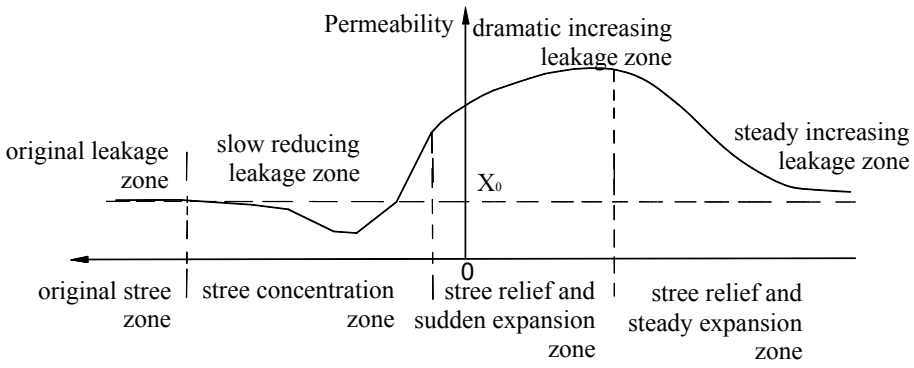

Fig. 15. Variation of permeability and seepage zones in the floor of the protective layer

3.5. Field verification

Deformation, gas pressure and gas flow quantity from boreholes in the protected seam $F_{16,17}$ were tested during extraction of the protective layer F_{15}, test results are shown in Fig. 16. In Fig. 16, the horizontal axis stands for the distance between test points and working face, the distance is zero when working face is extracted to test points, the sign convention is positive when working face is extracted back test points. The results from Fig. 16 are as follows:

(1) The original stress zone of the protected seam $F_{16,17}$ is located at 30 m at the front of the working face. In this zone, the stratum were not effected by mining, under normal stress, gas parameters keep their original values, gas emission rate from borehole reduce naturally in negative exponent rule. This zone belongs to gas original seepage zone.

(2) The stress concentration zone of the protected seam $F_{16,17}$ is located within the distance of 5 m and 30 m at the front of the working face, maximum compressive deformation value 0.5‰. The cracks and pores in the coal were closed and shrank owing to concentrating stress, gas permeability get worse and worse ,and gas flow which originally is little tend towards reduction. This zone belongs to gas speed-down and reduction zone.

(3) Stress of protected coal seam $F_{16,17}$ begin to be released when the working face is extracted to about 5 m at the front of test point, and the expansion deformation rate accelerates.

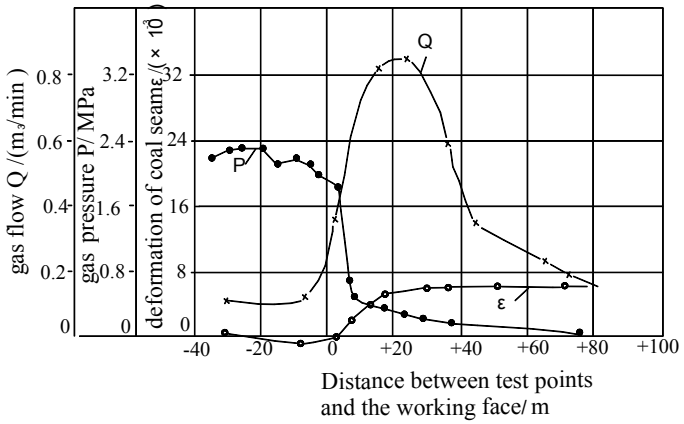

Fig. 16. Deformation, gas pressure and gas flow quantity in seam $F_{16,17}$ during extraction of the protective layer

The gas content in the protective layer F_{15}-23220 mining area was measured for more than 10 locations; all the measured gas contents were higher than 20%. It proved that the significant stress reduction in the floor stratum resulted in the formation of a large amount of inter-seam fractures and bed-separation fractures. Hence, the gas permeability coefficient was increased remarkably. A large quantity of gas was desorbed in the protected seam and flowed into the mining area in the protective layer. The expansion deformation value was maximum 0.6‰ when test point locates within 30~40 m behind the working face. The cracks are formed in the stratums going with pressure relief, gas desorbed is discharged via cracks between the seams, gas pressure is reduced form 2.1 MPa to the value of atmospheric pressure, and the gas flow increased rapidly. The gas flow get its maximum value 0.5~1.0 m^3/min when test borehole locates within 30~40 m behind the working face. This zone belongs to sharp speed-up and increment zone.

(4) The fallen rocks in the goaf are compacted gradually when the distance is about 40 m behind the working face, stratums and coal seam bear pressure once more, but the stress is less than the original stress, the coal seam still has some expansion deformation, gas has been already in the exhaustion situation due to natural emission and artificial drainage.

4. Conclusions

On the basis of full consideration of rock heterogeinity and in combination with gas geology at Pingdingshan Mine 5, a numerical model was estalished with the gas-solid coupling rock failure process analysis system RFPA-Gas to simulate the stress variation law, roof and floor deformation, fracture evolution law, displacement in the protected seam, change in gas permeability and gas migration law during protective layer extraction. The following conclusions can be drawn:

(1) The simulation results reproduced the stress variations in coal and rock strata, roof and floor deformation and fracture evolution process during protective layer extraction. The movement of rock strata were characterized by upper three zones and lower two zones:

caving zone, fracture zone and bending subsidence zone in the vertical direction in the overlying strata; floor deformation and failure zone and elasto-plastic deformation zone in the vertical direction in the underlying strata.

(2) During extraction of the protective layer, stress relief led to vertical and horizontal displacements in the protected seam. The maximum vertical and horizontal displacements reached 154 mm and 58.2 mm, respectively. The gas permeability coefficient changed from 0.002 m^2/MPa^2d to 5 $m^2/MPa^2 \cdot d$, which increased by 2500 times. A large amount of desorbed gas flowed into the protective layer through inter-seam fractures. Hence, the outburst threat in the protected seam was eliminated.

(3) By comprehensive analysis of stress variation, deformation characteristics and fracture distribution, and with consideration of gas seepage rate, gas pressure and variation of gas permeability, according to gas leakage rate, the floor stratum below the protecive layer was divided into four leakage zones. They corresponded to four zones with different stress states and fracture development: original leakage zone (original stress zone) - slow reducing leakage zone (stress concentration zone) – dramatic increasing leakage zone (stres relief and sudden expansion zone) – steady increasing leakage zone (stress relief and steady expansion zone). Among them, the stress relief and sudden expansion zone referred to the region between the vertical fracture and horizontal bed separation fracture in the floor, i.e., the region between the compressive-shear fracture below coal wall and micro-fracture in the goaf area. Under large gas pressure gradient, this region is highly prone to gas outburst and is the key area for gas control. The stress relief and steady expansion zone was located in the horizontal fracure zone due to floor heave, correspoding to tensile failure zone in the floor stratum.

(4) The simulation results were compared with the stress-relief effects in the field. The results are verified and in good agreement with the measured results.

Acknowledgements

The study is financially supported by Key Program of National Natural Science Foundation of China (Grant no. 50534070, 40638040).

References

Cheng Y.P., Yu Q.X., Yuan L., 2003. *Gas extraction techniques and movement properties of long distance and pressure relief rock mass upon exploited coal seam*. Journal of Liaoning Technical University, 8, 22(4):483-486.

Elune, 1992. *Prediction and control Dynamic Phenomenon of Gas in Coal Mine*. Tang X.Y., Song D.S., Wang R.L. Translation. Beijing: China Coal Industry Publishing House.

Jia T.R., 2006. *Study on gas control technology with mining close-range protective seam in Pingdingshan coal district*. M.S. Thesis, Jiaozuo: Henan Polytechnic University.

Liu Z.G., Yuan L., 2006. *Study on Gas Extracting Technology of Gas Destressing and Gas Storage from Fractures in Surrounding Rock of Roof and Floor of the First-mined Seams*. China Coalbed Methane, 3(2):11-15.

Shi B.M., Yu Q.X., Zhou S.N., 2004. *Numerical simulation of far-Distance rock strata failure and deformation caused by mining protecting stratum*. Journal of China University of Mining & Technology, 33(3):259-263.

Valliappan S., Zhang W.H., 1996. *Numerical modeling of methane gas migration in dry coal seams*. International Journal for Numerical and Analytical Methods in Geomechanics, 20(8):571–593.

Wang L.J., Wang Y., Sun B.J. et al., 2008. *Numerical Simulation Analysis on Coal and Rock Fracture Distribution after Extraction of Protective Seam in Hong Ling Coal Mine*. Mining Safety & Environmental Protection, 5, 1-3, 5.

Yang D.M., 1992. Analysis for effect on extration of Lower Release Seam. Xuzhou: China University of Mining and Technology.

Yang D.M., Yu Q.X., 1988. *Study of the Earth Stress Variation after Extraction of Lower Release Seam in Gently Inclined Strata*. Journal of China University of Mining & Technology, (1):32-38.

Yang T.H., Tang C.A., Xu T. et al., 2004. *Seepage Characteristic in Rock Failure—Theory, Model and Applications[M]*. Beijing: Science Press.

Yu B.F., 2004. *Theory and practice of protective seam*. China Coal Industry Publishing House.

Received: 12 August 2011